Computational methods in engineering sciences, vol. 1, no. 4, Winter 2024 Serial no. 4
DOI: 10.22034/cmes.2024.2020680.1020

The effect of channel inlet angle on the square gas cyclone performance: A Numerical Study

F. Parvaz [1], J. Foroozesh [2], N. Uygur Babaoğlu [3], S. H. Hosseini [4,*], G. Ahmadi [5] and K. Elsayed [6]

[1] Department of Mechanical Engineering, Semnan University, P.O. Box 35131-191, Semnan, Iran
[2] Department of Metallurgy and Materials Science, Faculty of Engineering, Shahid Bahonar University of Kerman, Kerman, Iran
[3] Department of Environmental Engineering, Kahramanmaras Sutcu Imam University, Kahramanmaras, Turkey
[4] Department of Chemical Engineering, Ilam University, Ilam 69315–516, Iran
[5] Department of Mechanical and Aerospace Engineering, Clarkson University, Potsdam, NY 13699-5725, USA
[6] Mechanical Power Engineering Department, Faculty of Engineering - Mataria, Helwan University, Masaken ElHelmia P.O. Cairo 11718, Egypt

* Corresponding Author

Received: 18/01/2024, Revised: 07/02/2024, Accepted: 27/02/2024.

Abstract
The gas cyclones have been widely used in various industries to remove solid particles in different sizes and densities from gas streams. The current work investigated the effect of inlet angle on the flow patterns and the gas cyclone performance using Computational Fluid Dynamics (CFD). For the simulation of the continuous phase, Reynolds Stress Modeling (RSM) was used to evaluate the airflow behavior inside square gas cyclones. The collection efficiency was evaluated for different inlet angles using the one-way coupling assumption. The presented results indicated that the best angle is 60 than the rest of angle and 30 degrees has less pressure drop than other cases. The minimum and maximum turbulence intensities occur at the inlet and the inner vortex finder. Increasing inlet velocity leads to improvement in the collection efficiency and the best angle of tangential inlet is 60 degrees, which has the best grade efficiency cure than other angles.

Keywords
Square gas cyclone, CFD simulations, inlet angle effects.

1. Introduction

A Gas cyclones have been widely used in industries to remove solid particles of different sizes and densities from gas streams [1]. Owning to low cast, small size and flexibility, their aim is to separate particles to reduce air pollution on industrial scales. Collection efficiency and pressure drop are two major factors, which can help design and usage of them. With the help of centrifugal force, separation occurs in a gas cyclone. Coarse particles toward to wall after moving to the dustbin, but fine particle exit through the tube [2–7]. Generally, gas cyclones are divided into conventional and square. While most cyclones are circular, square gas cyclones have been used in the Circulating Fluidized Beds (CFB). One drawback of circular cyclones is the enormous volume and dense refractory, which have responsibility for the stop time and long start. The volume of the square cyclone is somewhat less than a conventional cyclone, and the stop and start time can be simply integrated by the boiler [3,8]. The collection efficiency of the square cyclone is typically lower than the circular ones. Hence, there is an interest in developing methods to improve the collection efficiency of industrial square cyclones. Fatahian et al. [6] conducted the effect of laminarizer on cyclone performance. They showed that using it can improve collection efficiency than Stairmand gas cyclone. In addition, Huang et al. [9] enhanced the collection efficiency of the cylindrical gas cyclone by means of laminarizer that increase 50 percent of cut of size diameter of performances obtained from the laminarizer. Wasilewski et al. [3] investigated the effect of changing the diameter of the exit tube and its addition length on gas cyclone performance. They reported that these changes have a considerable effect on gas cyclones. Safikhani et al.[4] estimated pressure drop and collection efficiency in a square gas cyclone with the help of CFD techniques, which was compared with the experimental data of Wang et al. [8] and in order to validate, the numerical result compared with Raoufi et al. [7]. They optimize geometrical parameters such as up length, down length, and the diameter of vortex finder. Their results showed that Pareto approach in better than neural network. Although many investigations have been conducted to increase collection efficiency with varying geometrical parameters [10–13]. Few works have been performed on impact of inlets on collection efficiency. Hosseini [14] has assessed the shape of the inlet of the square gas cyclone. Results showed that increasing inlet velocity can lead to increasing pressure drop and collection efficiency in the inclined inlet. In the present work, we studied the effect of inlet angle on flow pattern, collection efficiency, and erosion rate of square cyclones. The ANSYS-FLUENT commercial software was used in the simulations. The RSM model was used to simulate

DOI: 10.22034/cmes.2024.2020680.1020

the gas stream inside the square gas cyclones. In addition, the one-way coupling assumption was made in that the gas flow carries the particles, but the effect of particles on the gas flow is negligible. The corresponding collection efficiencies of gas cyclones for different particle sizes were evaluated.

2. CFD model

In this section, the governing equations used in the simulations airflow and particle trajectory analysis are presented.

2.1. Turbulence model

The airflow in cyclones is typically in a turbulent state of motion. For an incompressible flow, the continuity and momentum equations are written as [15],

$$\frac{\partial \overline{u_i}}{\partial x_i} = 0 \tag{1}$$

$$\frac{\partial \overline{u_i}}{\partial t} + \overline{u}_j \frac{\partial \overline{u_i}}{\partial x_j} = -\frac{1}{\rho}\frac{\partial \overline{P}}{\partial x_i} + \nu \frac{\partial^2 \overline{u_i}}{\partial x_i \partial x_j} - \frac{\partial}{\partial x_j} R_{ij} \tag{2}$$

where $\overline{\mu_i}$ is the mean velocity vector, x_i is the position vector, $\overline{P}$ is the mean pressure, ρ is the gas density, v is the gas kinematic velocity, and $R_{ij} = \overline{u_i' u_j'}$ is the Reynolds stress tensor. Here $u_i' = u_i - \overline{u_i}$ is the *i*th fluctuating velocity component.

Previous studies investigated the importance of turbulence models for predicting swirling flows [13,16,25–28,17–24,32]. They showed that the Reynolds Stress Modeling (RSM) is able to predict the behavior of the complicated swirling flows. Therefore, the RSM was used in current simulations to investigate the effect of the inlet angle.

The RSM turbulence model provides the transport equations for evaluating turbulence stresses. That is,

$$\frac{\partial}{\partial t} R_{ij} + \overline{u_k} \frac{\partial}{\partial x_k} R_{ij} = \frac{\partial}{\partial x_k}\left(\frac{\nu_t}{\sigma^k}\frac{\partial}{\partial x_k} R_{ij}\right) - \left[R_{ik}\frac{\partial \overline{u_j}}{\partial x_k} + R_{jk}\frac{\partial \overline{u_i}}{\partial x_k}\right] - C_1 \frac{\varepsilon}{k}\left[R_{ij} - \frac{2}{3}\delta_{ij} K\right] - C_2\left[P_{ij} - \frac{2}{3}\delta_{ij} P\right] - \frac{2}{3}\delta_{ij}\varepsilon \tag{3}$$

where the turbulence production term P_{ij} is given as,

$$P_{ij} = -\left[R_{ik}\frac{\partial \overline{u_j}}{\partial x_k} + R_{jk}\frac{\partial \overline{u_i}}{\partial x_k}\right], \quad P = \frac{1}{2} P_{ij} \tag{4}$$

here P stands for the fluctuating kinetic energy production, V_t is the turbulence (eddy) kinematic viscosity, and the empirical constants are $\sigma^k = 1, C_1 = 1.8, C_2 = 0.8$.

The transport equation for the turbulence dissipation rate, ε, is given as,

$$\frac{\partial \varepsilon}{\partial t} + \overline{u_j}\frac{\partial \varepsilon}{\partial x_j} = \frac{\partial}{\partial x_j}\left[\left(\nu + \frac{\nu_t}{\sigma^\varepsilon}\right)\frac{\partial \varepsilon}{\partial x_j}\right] - C^{\varepsilon 1}\frac{\varepsilon}{K} R_{ij}\frac{\partial \overline{u_i}}{\partial x_j} - C^{\varepsilon 2}\frac{\varepsilon^2}{K} \tag{5}$$

where $k = \frac{1}{2}\overline{u_i' u_j'}$ is the fluctuating kinetic energy. The values of constants are $\sigma^\varepsilon = 1.3,\ \sigma^{\varepsilon 1} = 1.44,\ \sigma^{\varepsilon 2} = 1.92$.

2.2. Discrete Phase Modeling (DPM)

The particle equation of motion is used to track particle trajectories through airflow. Due to the dilute nature of the flow, the interaction between solid particles is ignored. Particle movement can be determined using Newton's second law. For spherical particles considering the hydrodynamic drag force and gravity, the governing equation of motion is written as [29],

$$\frac{dx_p}{dt} = u_p \tag{6}$$

$$\rho_P \frac{d\vec{u}}{dt} = \frac{3\rho}{4 d_P} C_D \left|\vec{u} - \overrightarrow{u_P}\right|\left(\vec{u} - \overrightarrow{u_P}\right) + \frac{g_i\left(\rho_p - \rho\right)}{\rho_p} \tag{7}$$

Here, the drag coefficient C_D is given as,

Table 2. Size of different parts.

	D	D_e	h	H	B	a	a′	h′
Dimension (mm)	2000	100	400	800	50	150	75	240

$$C_D = \begin{cases} \dfrac{24}{\mathrm{Re}_p} & \mathrm{Re}_p < 0.1 \\ 24\left(1 + 0.15\,\mathrm{Re}_p^{\,0.687}\right) & 0.1 < \mathrm{Re}_p \le 1000 \\ 0.44 & \mathrm{Re}_p > 1000 \end{cases} \tag{8}$$

2.3. Geometry and Grid generation

The numerical studies were conducted on four square gas cyclones with different inlet channel angles, as shown in Fig. 1. The angles analyzed include 30, 45, 60, and 90 degrees. Table 2 provides the specific geometrical dimension details.

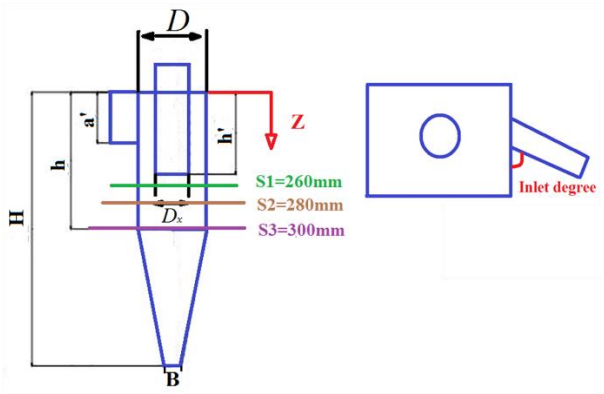

Fig. 1. Square gas cyclone characteristics.

The different sections across the cyclone, namely S1, S2, and S3, are measured as distances from the top of the cyclone. The 3-D structured grids were generated for all square cyclone models. A sample surface grid is shown in Fig. 2. The investigation of the grid independence was conducted by comparing the values of static pressure and

DOI: 10.22034/cmes.2024.2020680.1020

total pressure, which are obtained from different mesh sizes. Three different meshes with coarse, medium, and fine grids are tested, and the calculated pressure drop and total pressure are listed in Table 3.

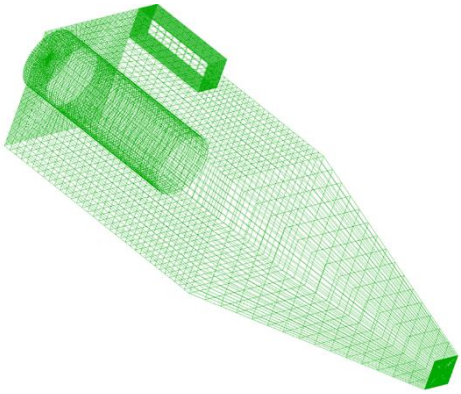

Fig. 2. The computational grids used in the simulations.

Table 3. The results of different grids.

Number of cells	Pressure drop	Total Pressure
191984	208.71	185.63
296904	221.95	193.65
349464	222.56	199.86
[a]%Difference	6.6	7.66

[a] The percentage variance between the coarsest and finest grid.

Table 3 displays the pressure drop variations observed across three grid sizes: 191984, 296904, and 349464 hexahedral cells. The corresponding percentage differences among these grids, as shown in Table 4, suggest that the CFD results obtained using 296904 cells are essentially independent of the grid resolution.

2.4. Boundary conditions and solver setting

The inlet velocity and turbulence intensity (TI) (up to 5%) were specified at the tangential channel inlet. The boundary condition at the outlet tube was an outflow condition. Furthermore, all walls are set with no-slip velocity. In addition, the particle trap condition at the cyclone walls was assumed to calculate collection efficiency. The ANSYS-FLUENT 22 CFD code was employed in the current work to simulate the gas flow inside the square cyclones. Table 4 shows the discretization schemes used for different parameters. The standard wall function was used to consider the turbulent effect on the wall. First, all solutions were obtained for the steady state flow condition. Then, the unsteady simulations were performed using the steady solution as the initial condition. The resident time was determined for the cyclone gas flow rate [30].

Table 4. Used discretization schemes.

Scheme	Numerical sitting
Body force weighted	Pressure discretization
SIMPLE	Pressure velocity coupling
QUICK	Momentum discretization
Second-order upwind	Turbulent kinetic energy
Second-order upwind	Turbulent dissipation rate
First-order upwind	Reynolds stress

2.5. Model validation

Su and Mao [31] conducted a set of experiment to study the flow of gas-solid suspension within a square cyclone separator. Their square gas cyclone was a cube, tetrahedron pyramid, tangential channel, and outlet pipe. To validate the current computational model, the cyclone operated by Su and Mao [31] was simulated across a range of inlet velocities and particle sizes. Fig. 3 exhibits the comparison between the predicted collection efficiency and pressure drops, obtained from the simulation results, with the experimental data provided by Su and Mao [31]. The results demonstrate a strong agreement between the simulation and experimental data.

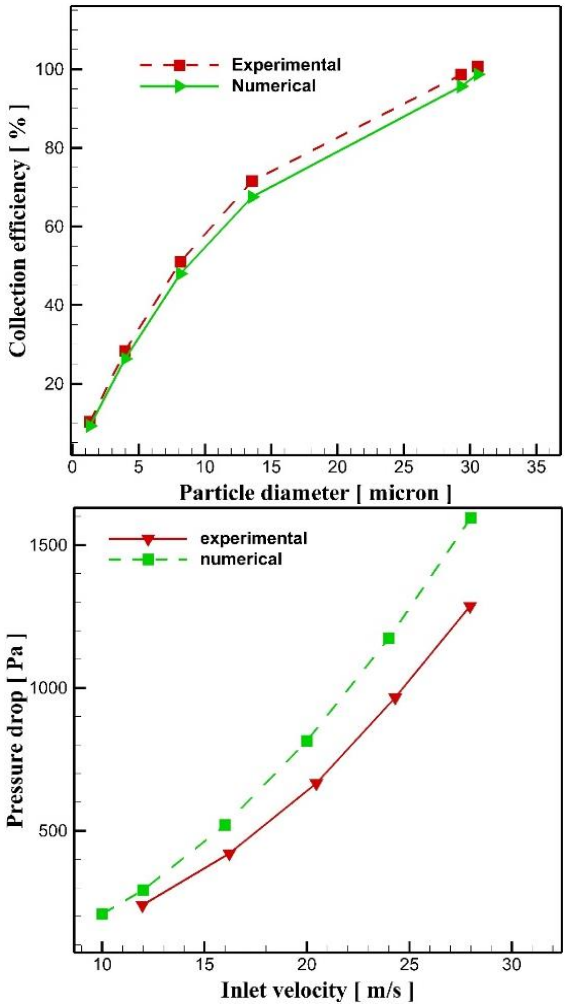

Fig. 3. The computational grids used in the simulations.

3. Results and discussion

This section describes the simulation results. The variation of tangential velocity, turbulence intensity, axial velocity, pressure drop, and collection efficiency for different conditions are discussed.

3.1. Tangential velocity

The tangential and axial velocities affect the trajectory of solid particles and the gas cyclone performance. In particular, the tangential velocity is the critical parameter influencing the collection efficiency. Also, there is a strong connection between pressure drop and tangential velocity. Generally, the tangential velocity profile can be

DOI: 10.22034/cmes.2024.2020680.1020

divided into two regions: free vortex and forced vortex. In Fig. 4, the radial velocity profiles across different sections of the cyclone and inlet channel angles are depicted for an inlet velocity of 20 m/s. Starting from the center of the gas cyclone, the tangential velocity progressively increases, forming what is known as the forced vortex, until it reaches the top. Following this, the tangential velocity decreases, creating the free vortex. These two vortices are commonly referred to as Rankine vortices. As shown in Fig. 4, the tangential velocity profiles exhibit an M-shape in the radial direction.

By examining the various locations indicated in Fig. 4, it becomes evident that increasing the inlet angle leads to a decrease in tangential velocity. This reduction in tangential velocity can have an impact on the collection efficiency. Specifically, the maximum tangential velocity corresponds to an inlet angle of 60 degrees, while the minimum tangential velocity occurs at an inlet angle of 30 degrees. Notably, in the case of a 90-degree inlet angle, the maximum tangential velocity is observed specifically near the cyclone wall, distinguishing it from the other cases. In overall, Fig. 4 suggests that altering the inlet angle can either enhance or diminish both the tangential velocity and the collection efficiency.

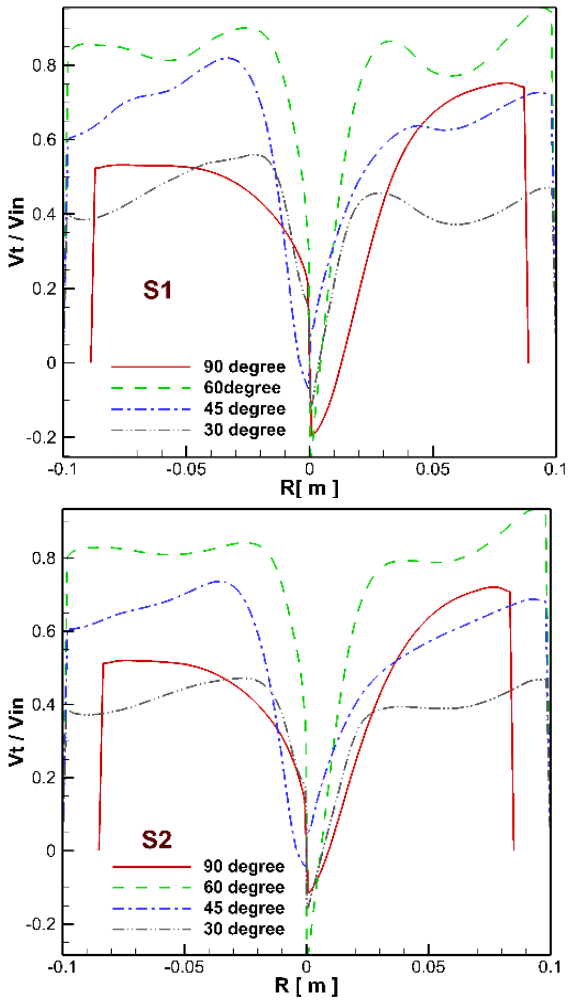

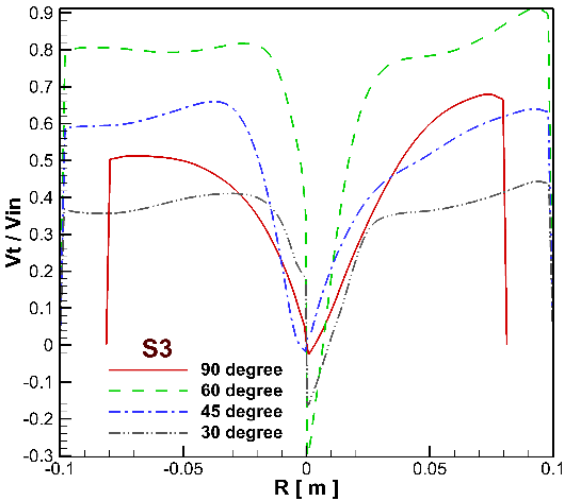

Fig. 4. The tangential velocity on different sections of the cyclone for different inlet channel angles.

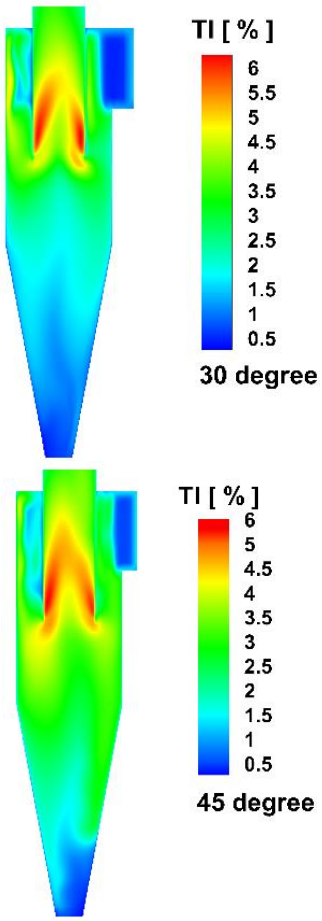

DOI: 10.22034/cmes.2024.2020680.1020

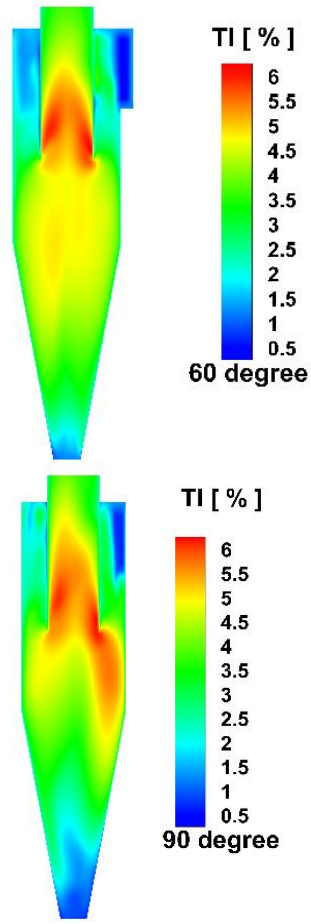

Fig. 5. Distribution of Turbulent intensity for different inlet channel angles.

3.2. Turbulent Intensity

The contour plot of Turbulent Intensity (TI) on the mid-section (X=0) for different inlet angles and V=20 m/s are shown in Fig. 5. It is seen that the minimum value of turbulence intensity occurs at the bottom of the gas cyclone, namely the end of the tetrahedron pyramid part. In this region, the gas flow is stagnant. The maximum turbulence intensity is observed in the vicinity of the internal wall of all vortex finders. This could adversely affect the collection efficiency by dispersing solid particles, some of which may enter the vortex finder and exit through the gas outlet.

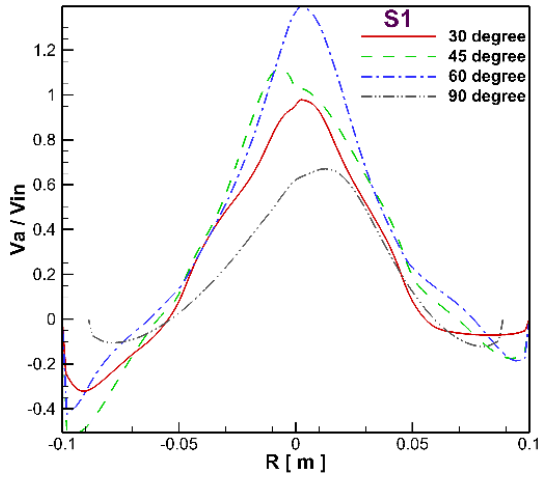

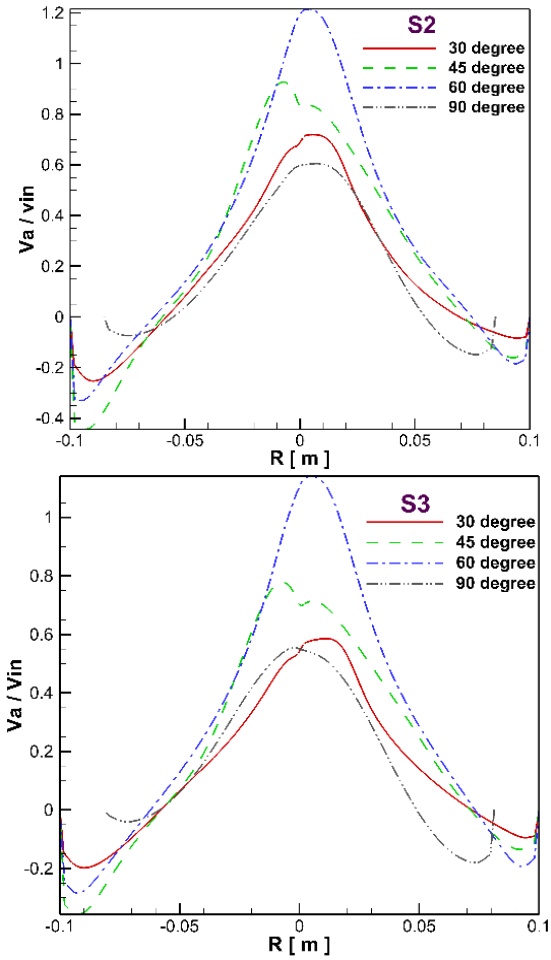

Fig. 6. The axial velocity on different sections of the cyclone for different inlet channel angles.

3.3. Axial velocity

The axial velocity within gas cyclones is typically divided into two distinct regions: the downward flow and the upward flow. The downward flow aids in directing particles towards the bottom of the cyclone cone, facilitated by the gas boundary layer. Conversely, the upward flow is responsible for lifting fine particles upwards. Fig. 6 shows the axial velocity on different sections of the cyclone for different inlet channel angles for V=20 m/s. As depicted in Fig. 6, it can be observed that the highest magnitude of upward flow is associated with the 60-degree inlet angle. This can be attributed to the pronounced swirl flow pattern of the axial velocity, resembling an inverted V shape.

As shown in Fig. 6, a comparison of axial velocities reveals that the inlet angles have a significant impact on the swirl flow within the central region of the gas cyclone. This change in swirl flow is influential in determining the collection efficiency of the gas cyclone.

3.4. Pressure drop

Fig. 7 shows the static pressure distribution overall of gas cyclone on the mid-section (X=0). In general, the static pressure is higher near the wall than in the central parts. Furthermore, negative static pressure occurs inside and beneath the outlet tube. It has been observed that the effect of channel angle can impact the static pressure. Increasing the angle of a channel can indeed cause the pressure drop to decrease next to the walls. In general, as

DOI: 10.22034/cmes.2024.2020680.1020

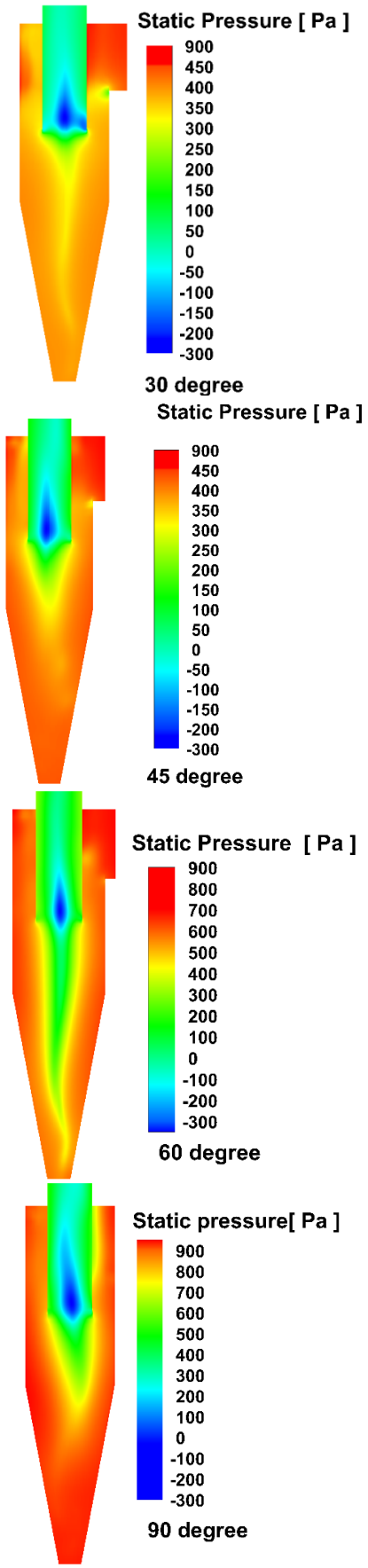

Fig. 7. Counters the static pressure (V=20 m/s).

the angle of the channel increases, the flow experiences a reduction in the frictional resistance against the channel walls, resulting in a lower pressure drop. Furthermore, it has been observed that a channel with a 30-degree angle tends to have a lower pressure drop compared to channels with other angles. This lower pressure drop translates to a reduction in energy losses associated with fluid flow through the channel. Consequently, systems utilizing a 30-degree channel configuration may benefit from improved energy efficiency.

3.5. Collection efficiency

The collection efficiency was written by η as follows:

$$\eta = \left(1 - \frac{n_{out}}{n_{total}}\right) \times 100 \qquad (9)$$

In equation 9, n_{out} is the number of particles that escaped through the exit tube, and n_{total} is the number of particles injected into the gas cyclone from the inlet.

As shown in Figure 10, the collection efficiency demonstrates improvement as the inlet velocity increases, which subsequently leads to an increase in the cut size diameter. Additionally, a larger particle size corresponds to a higher collection efficiency. In summary, coarse particles exhibit higher collection efficiency compared to fine particles. Furthermore, except for an angle of 90 degrees, increasing the inlet angle also leads to an increase in the collection efficiency.

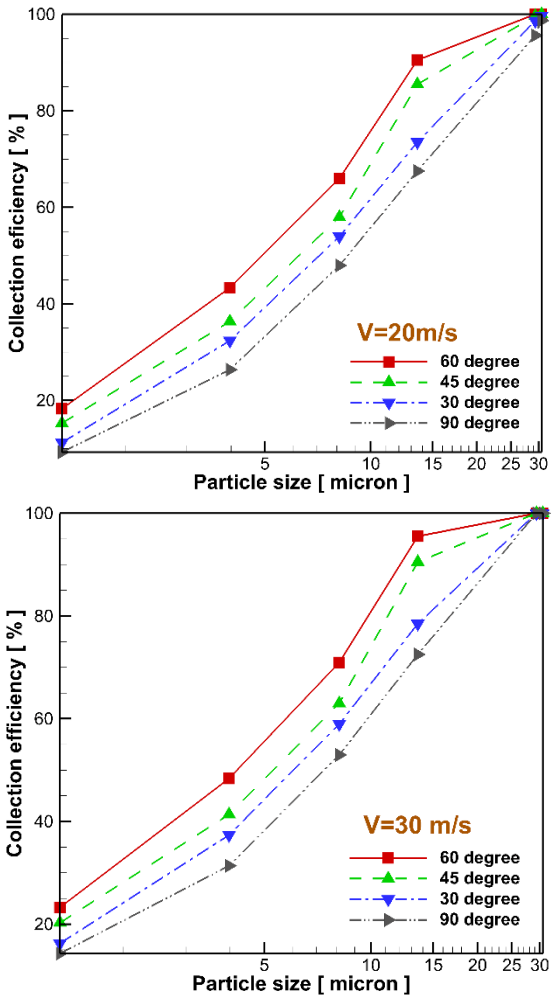

DOI: 10.22034/cmes.2024.2020680.1020

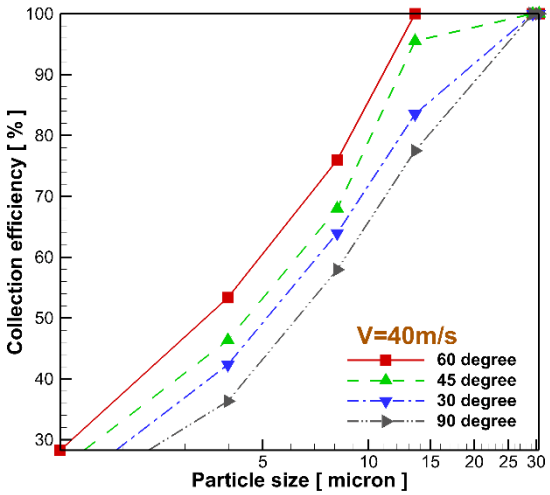

Fig. 8. Collection efficiency for different inlet velocities and inlet angles.

From the CFD results illustrated in Figs. 4 and 5 for inlet angles of 30 and 90 degrees, it is apparent that the collection efficiency is more significantly influenced by the turbulent intensity rather than the tangential velocity.

4. Conclusions

In this study, we conducted simulations to examine the airflow patterns within square cyclones and evaluate their performance across various inlet angles. The ensuing results provided the following insights into the relationship between inlet angles and cyclone performance:

- By varying the inlet angle within different ranges, it was observed that the 60-degree inlet angle exhibited the highest tangential velocity compared to the other angles.
- A 30-degree angle exhibited a lower pressure drop compared to channels with other angles.
- When considering a 60-degree inlet angle, it was observed that the axial velocity was higher compared to other cases.
- Inside the exit tube, a negative pressure drop was observed. However, the walls of the gas cyclone experienced higher pressure drops compared to other regions, and they were found to be sensitive to changes in the inlet angle.

References

[1] F. Parvaz, S.H. Hosseini, A.R. Bastan, J. Foroozesh, N.U. Babaoğlu, K. Elsayed, G. Ahmadi, Influence of gas exhaust geometry on flow pattern, performance, and erosion rate of a gas cyclone, Korean J. Chem. Eng. 40 (2023) 1587–1597. https://doi.org/10.1007/s11814-023-1430-2.

[2] Y. Su, The turbulent characteristics of the gas-solid suspension in a square cyclone separator, Chem. Eng. Sci. 61 (2006) 1395–1400. https://doi.org/10.1016/j.ces.2005.09.002.

[3] M. Wasilewski, L.S. Brar, G. Ligus, Experimental and numerical investigation on the performance of square cyclones with different vortex finder configurations, Sep. Purif. Technol. 239 (2020) 10–24. https://doi.org/10.1016/j.seppur.2020.116588.

[4] H. Safikhani, M.A. Akhavan-Behabadi, N. Nariman-Zadeh, M.J. Mahmood Abadi, Modeling and multi-objective optimization of square cyclones using CFD and neural networks, Chem. Eng. Res. Des. 89 (2011) 301–309. https://doi.org/10.1016/j.cherd.2010.07.004.

[5] H. Fatahian, E. Fatahian, M. Eshagh Nimvari, G. Ahmadi, Novel designs for square cyclone using rounded corner and double-inverted cones shapes, Powder Technol. 380 (2021) 67–79. https://doi.org/10.1016/j.powtec.2020.11.034.

[6] H. Fatahian, E. Fatahian, M.E. Nimvari, Improving efficiency of conventional and square cyclones using different configurations of the laminarizer, Powder Technol. 339 (2018) 232–243. https://doi.org/10.1016/j.powtec.2018.08.038.

[7] A. Raoufi, M. Shams, H. Kanani, CFD analysis of flow field in square cyclones, Powder Technol. 191 (2009) 349–357.

[8] S. Wang, M. Fang, Z. Luo, X. Li, M. Ni, K. Cen, Instantaneous separation model of a square cyclone, Powder Technol. 102 (1999) 65–70.

[9] A.-N. Huang, N. Maeda, D. Shibata, T. Fukasawa, H. Yoshida, H.-P. Kuo, K. Fukui, Influence of a laminarizer at the inlet on the classification performance of a cyclone separator, Sep. Purif. Technol. 174 (2017) 408–416.

[10] S. Venkatesh, R. Suresh Kumar, S.P. Sivapirakasam, M. Sakthivel, D. Venkatesh, S. Yasar Arafath, Multi-objective optimization, experimental and CFD approach for performance analysis in square cyclone separator, Powder Technol. 371 (2020) 115–129. https://doi.org/10.1016/j.powtec.2020.05.080.

[11] H. Fatahian, E. Hosseini, E. Fatahian, CFD simulation of a novel design of square cyclone with dual-inverse cone, Adv. Powder Technol. 31 (2020) 1748–1758. https://doi.org/10.1016/j.apt.2020.02.007.

[12] D.K. Le, J.Y. Yoon, Numerical investigation on the performance and flow pattern of two novel innovative designs of four-inlet cyclone separator, Chem. Eng. Process. - Process Intensif. 150 (2020) 107867. https://doi.org/10.1016/j.cep.2020.107867.

[13] F. Parvaz, S.H. Hosseini, G. Ahmadi, K. Elsayed, Impacts of the vortex finder eccentricity on the flow pattern and performance of a gas cyclone, Sep. Purif. Technol. 187 (2017) 1–13. https://doi.org/10.1016/j.seppur.2017.06.046.

[14] E. Hosseini, Performance assessment of a square cyclone influenced by inlet section modifications, J. Brazilian Soc. Mech. Sci. Eng. 42 (2020). https://doi.org/10.1007/s40430-020-02606-w.

[15] K. Elsayed, C. Lacor, The effect of cyclone inlet dimensions on the flow pattern and performance, Appl. Math. Model. 35 (2011) 1952–1968.

[16] F. Parvaz, S. Hossein, K. Elsayed, G. Ahmadi, Separation and Puri fi cation Technology Numerical investigation of e ff ects of inner cone on fl ow fi eld , performance and erosion rate of cyclone separators, 201 (2018) 223–237. https://doi.org/10.1016/j.seppur.2018.03.001.

[17] F.Parvaz, R.Rafee, F.Tallebi, Effects of the Outlet Pipe Diameter on the Performance of Aerocyclone

in Gas Droplet Two-Phase Flow, J. Mech. Eng. 48 (2018) 45–53.
[18] S.M. Vahedi, F. Parvaz, R. Rafee, M.K. Bakavoli, Journal of Heat and Mass Transfer Research Computational fluid dynamics simulation of the flow patterns and performance of conventional and dual-cone gas-particle cyclones, 4 (2018) 27–38. https://doi.org/10.22075/jhmtr.2017.1503.1100.
[19] S.M. Vahedi, F. Parvaz, M. Khandan Bakavoli, M. Kamali, Surface roughness effect of on vortex length and efficiency of the gas-oil cyclone through CFD modelling, Iran. J. Oil Gas Sci. Technol. 0 (2018) 68–84. https://doi.org/10.22050/ijogst.2018.102377.1417.
[20] N.U. Babaoğlu, F. Parvaz, S.H. Hosseini, K. Elsayed, G. Ahmadi, Influence of the inlet cross-sectional shape on the performance of a multi-inlet gas cyclone, Powder Technol. 384 (2021) 82–99. https://doi.org/10.1016/j.powtec.2021.02.008.
[21] M. Izadi, A.M. Makvand, E. Assareh, F. Parvaz, Optimizing the Design and Performance of Solid-Liquid Separators, Int. J. Thermofluids. 5–6 (2020) 100033. https://doi.org/10.1016/j.ijft.2020.100033.
[22] J. Foroozesh, F. Parvaz, S.H. Hosseini, G. Ahmadi, K. Elsayed, N.U. Babaoğlu, Computational fluid dynamics study of the impact of surface roughness on cyclone performance and erosion, Powder Technol. 389 (2021) 339–354. https://doi.org/10.1016/j.powtec.2021.05.041.
[23] F. Parvaz, S.M. Vahedi, M. Khandan, E. Assareh, Numerical investigation of the effects of geometry variation on the flow pattern and performance of Gas-Particle cyclones, Iran. J. Mech. Eng. 19 (2017) 101–122.
https://doi.org/20.1001.1.25384775.1396.19.4.6.3.
[24] S.M. Vahedi, F. Parvaz, M. Kamali, H. Jafari Jebeli, Numerical Investigation of the Impact of Inlet Channel Numbers on the Flow Pattern, Performance, and Erosion of Gas-particle Cyclone, Iran. J. Oil Gas Sci. Technol. 7 (2018) 59–78. https://ijogst.put.ac.ir/article_57757.html.
[25] F. Kaya, I. Karagoz, A. Avci, Effects of surface roughness on the performance of tangential inlet cyclone separators, Aerosol Sci. Technol. 45 (2011) 988–995. https://doi.org/10.1080/02786826.2011.574174.
[26] I. Karagoz, F. Kaya, CFD investigation of the flow and heat transfer characteristics in a tangential inlet cyclone, Int. Commun. Heat Mass Transf. 34 (2007) 1119–1126.
https://doi.org/10.1016/j.icheatmasstransfer.2007.05.017.
[27] E. Dehdarinejad, M. Bayareh, F. Parvaz, S.H. Hosseini, G. Ahmadi, Performance analysis of a gas cyclone with a converging-diverging vortex finder, Chem. Eng. Res. Des. 193 (2023) 587–599. https://doi.org/10.1016/j.cherd.2023.04.012.
[28] E. Dehdarinejad, F. Parvaz, S.H. Hosseini, G. Ahmadi, K. Elsayed, To, Performance analysis of a gas cyclone with a dustbin inverted hybrid solid cone, Aerosol Sci. Technol. ISSN. 56 (2023) 587–599. https://doi.org/10.1016/j.cherd.2023.04.012.
[29] A.R. Lambert, P.T. O'shaughnessy, M.H. Tawhai, E.A. Hoffman, C.-L. Lin, Regional deposition of particles in an image-based airway model: large-eddy simulation and left-right lung ventilation asymmetry, Aerosol Sci. Technol. 45 (2011) 11–25.
[30] Nihan Uygur Babaoˇglu, F. Parvaz, J. Foroozesh, S. Hossein, Geometry optimization of axial cyclone for high performance and low acoustic noise, 427 (2023). https://doi.org/10.1016/j.powtec.2023.118738.
[31] Y. Su, Y. Mao, Experimental study on the gas – solid suspension flow in a square cyclone separator, 121 (2006) 51–58. https://doi.org/10.1016/j.cej.2006.04.008.
[32] Abdali A, Monjezi V. Machine Learning-based Flexible Link Robot Control. Computational methods in engineering sciences. 2023 Aug 23;1(2):12-7.